Performance Characteristics of an Extended Throat Flow Nozzle for the Measurement of High Void Fraction Multi-Phase Flows

J. R. Fincke
Lockheed Martin Idaho Technologies Company
Idaho National Engineering and Environmental Laboratory, USA

C. Ronnenkamp, D. Kruse, J. Krogue, D. Householder
Perry Equipment Corporation, USA

ABSTRACT

An extended throat flow nozzle has been examined as a device for the measurement of very high void fraction ($\alpha \geq 0.95$) multi-phase flows. Due to its greater density and partial contact with the wall, the equilibrium velocity of the liquid phase appreciably lags that of the lighter gas phase. The two phases are strongly coupled resulting in pressure drops across the contraction and in the extended throat that are significantly different than those experienced in single-phase flow. Information about the mass flow rates of the two phases can be extracted from the measured pressure drops. The performance of an extended throat flow nozzle has been evaluated under multi-phase conditions using natural gas and hydrocarbon liquids at 400 and 500 psi. Two hydrocarbon solvents were used as the test liquids, Isopar M® (sp = 0.79) and Aromatic 100® (sp = 0.87). These data are compared to prior air-water data at nominally 15 psi. The high and low pressure data were found to be consistent, confirming that the temperature, pressure, and size scaling of the extended throat venturi are correctly represented. This consistency allows different sized devices to be applied under different fluid conditions (temperature, pressure, gas and liquid phase composition, etc) with confidence.

INTRODUCTION

In recent years, the metering of multiphase fluid streams prior to separation using flow nozzles or other pressure drop devices[1] has received increased attention. Significant progress has been made in the metering of multiphase fluids by first homogenizing the flow in a mixer then metering the pseudo single phase fluid in a venturi in combination with the measurement of fluid density obtained by a gamma densitometer or other device. This approach relies on the successful creation of a homogenous mixture with equal phase velocities. Under these conditions the mixture approximates a single phase fluid with density $\bar{r} = a r_g + (1-a) r_l$ where α is the volume fraction of the gas phase, and ρ_k, k=g,l is the gas and liquid phase density, respectively. This technique works well for flows which, after homogenizing, the continuous phase is the liquid phase. While the upper limit of applicability of this approach is ill defined, it is generally thought that for void fractions greater than about 90-95% a homogenous mixture is difficult to create or sustain. The characteristic undisturbed flow regime in this high void fraction range is that of an annular or annular mist flow. The gas phase flows in the center of the channel while the dense liquid phase flows in a film on the inner surface of the channel. Depending on the geometry, pressure and the flow rates of each phase, significant amounts of the denser phase may also become entrained in the gas phase and be transported as dispersed

droplets. While the liquid generally occupies <5% by volume, the mass flow rate of the liquid can be comparable to that of the gas phase due to its greater density.

The presence of the liquid phase complicates the measurement, causing conventional meters, such as orifice plates or venturi meters, to overestimate the flow rate of the gas phase. Figures 1 and 2 illustrate this problem. The venturi meter used is of conventional design following ASME guidelines[2]. The upstream piping is 2 inch inside diameter and the throat diameter is 1.4 inch for a contraction ratio of β=0.7. The gas mass flow rate is obtained in the usual manner from

$$(1) \qquad m_g = \frac{AC_c Y}{\sqrt{1-\beta^4}}\sqrt{2\rho_g \Delta P}$$

where m_g is the gas mass flow rate, A is the area of the throat, ΔP the measured pressure differential, ρ_g the gas density at flow conditions, C_c the discharge coefficient (C_c=0.995), and Y is the expansion factor. The test pressure was 400 psi, the gas phase was dry pipeline natural gas and the liquid phase was Isopar M® a hydrocarbon solvent with specific gravity of 0.79. The test temperature was approximately 80 °F. The liquid mass loading, defined as m_l/m_g, ranged from a low of 1.4 % to a high of 30 %. And the corresponding void fraction ranged from 0.997 to 0.95. The test configuration, which is shown in Figure 8, will be described in more detail in the following section. Figure 2 is a comparison of the apparent gas mass flow rate to the reference gas mass flow rate obtained by metering the dry pipeline gas using a conventional orifice meter and flow computer, before the introduction of the liquid phase. The presence of the liquid phase clearly increases the pressure drop in the venturi and results in the meter over predicting the true gas mass flow rate. The resulting error, in percent of reading, is shown in Figure 2. The error in the gas mass flow rate measurement ranges from around 7 % of reading for a mass loading of 1.4 % to a maximum of 27 % for a mass loading of 30 %.

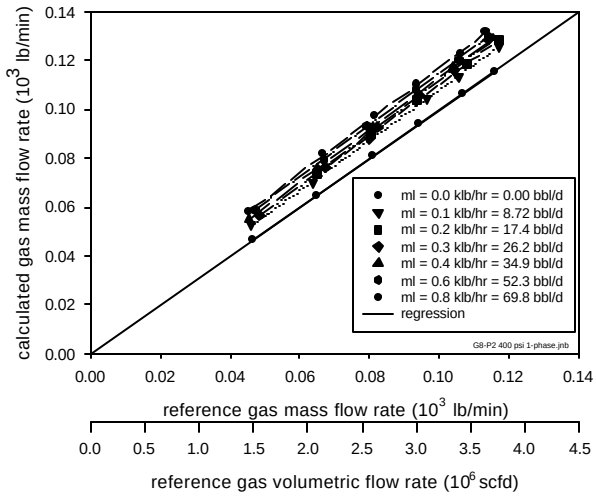

Figure 1. Venturi performance using the single phase calibration under multi-phase test conditions.

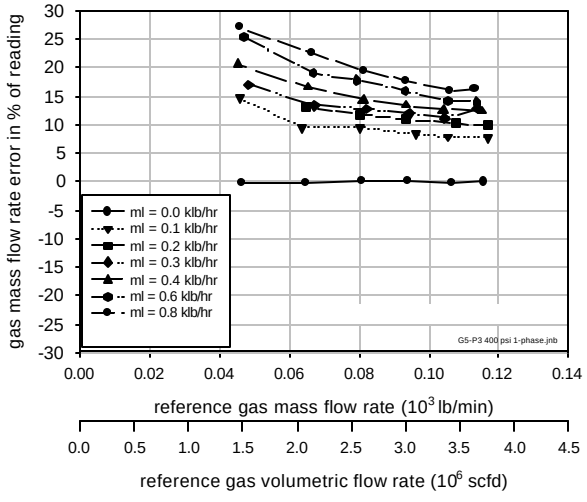

Figure 2. Mass flow rate error in percent of reading using single phase calibration under multi-phase test conditions.

The over prediction of the gas mass flow rate by the venturi meter is due to an increase in the pressure drop under multi-phase conditions. The increase in pressure drop is caused by the interaction between the gas and liquid phases. Liquid droplet acceleration by the gas, irreversible drag force work done by the gas phase in accelerating the liquid film and wall losses determine the magnitude of the observed pressure drop. The flow field is characterized and complicated by the continuous deposition and entrainment of liquid along the venturi length and by the presence of surface waves on the liquid film. The continuous deposition and entrainment process contributes to the overall pressure drop through the loss of momentum caused by the acceleration of the newly entrained droplets. The surface waves present an effectively roughened surface over which the gas must flow increasing the momentum loss due to the addition of form drag to the interfacial shear stress.

A simple, semi-empirical solution to the overestimation of gas mass flow rate under multi-phase conditions has been proposed by Murdock[3]. Murdock's analysis, which ignores any interaction (momentum exchange) between the gas and liquid phases yields an equation, which, if the ratio of gas to liquid mass flow rate is known *a priori*, proposes to correct the apparent reading to the actual value. The resulting equation is given below, where M is an empirically determined constant:

$$(2) \qquad m_{g(Murdock)} = \frac{m_{g(apparent)}}{1 + M\left(\frac{m_l}{m_g}\right)\frac{C_g Y}{C_l}\sqrt{\frac{\rho_g}{\rho_l}}}.$$

The subscript (*apparent*) denotes the value of m_g obtained from equation (1) under multi-phase conditions, and the subscript (*Murdock*) denotes the corrected value according to Murdock's equation. The C_k, k=g,l are the discharge coefficients for the gas and liquid phases respectively. Murdock[3] recommended a value of 1.26 for M. The results of applying equation 2 to the data of Figure 1 appear in Figures 3 and 4. The ratio of the liquid to gas mass flow rate used in equation 2 was taken from the measured values obtained by metering the single phase fluids independently before mixing. As seen in Figures 3 and 4 the correction is insufficient to adjust the apparent reading to the actual reference value.

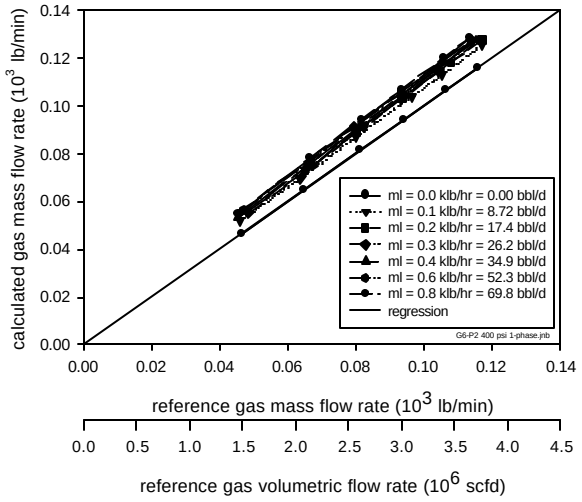

Figure 3. Venturi performance under multi-phase conditions using the Murdock correction, M=1.26.

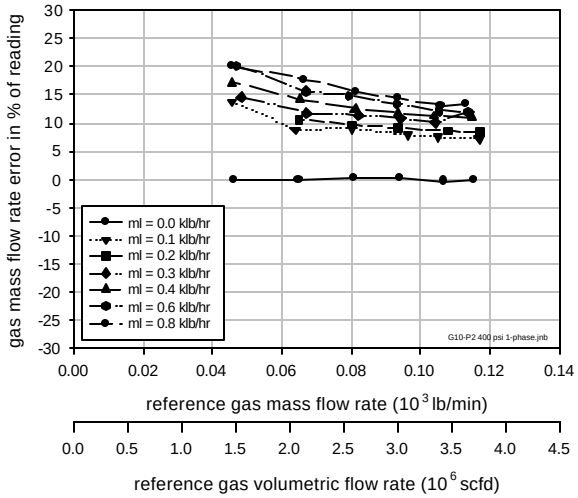

Figure 4. Gas mass flow rate error in percent of reading using the Murdock correction, M=1.26.

The approach suggested by Jamieson and Dickinson[4] was to adjust the value of M to fit the data. For the data examined here the value of M required to obtain agreement for the $\dot{m}_l$ = 100 lb/hr data is 25.2, twenty times the original recommended value of 1.26. The results of applying equation 2 to the data of Figure 1 using M = 25.2 appear in Figures 5 and 6. Clearly M is not a universal constant. While the $\dot{m}_l$ = 100 lb/hr data is adequately corrected the $\dot{m}_l$ > 100 lb/hr is significantly over compensated.

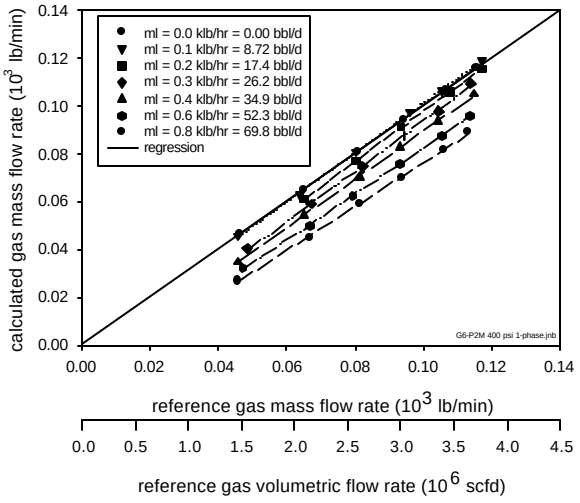

Figure 5. Venturi performance under multi-phase conditions using the Murdock correction, M=25.2.

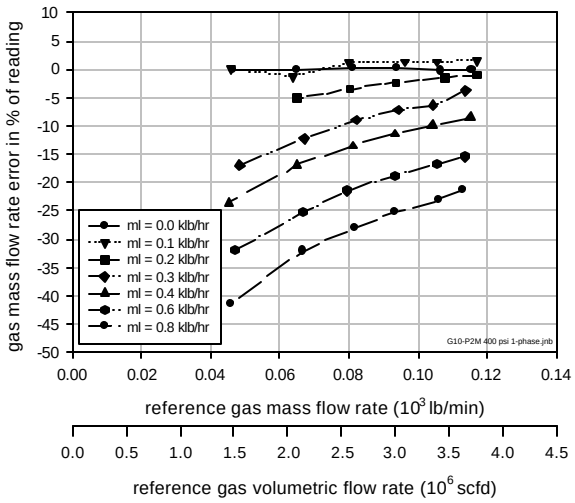

Figure 6. Gas mass flow rate error in percent of reading, using the Murdock correction, M=25.2.

Reliable metering of high void fraction multi-phase flows over a wide range of conditions (liquid loading, pressure, temperature, and gas and liquid composition) without prior knowledge of the liquid and gas mass flow rates requires a different approach than the simple modification of single phase meter readings. Conceptually, a method of metering such a flow is to impose an acceleration or pressure drop on the flow field via a constriction or expansion and to observe the pressure response of the device at several locations. Because the multi-phase pressure response differs significantly from that of a single-phase fluid, it is likely that the measured differentials will be a unique function of the mass flow rates of each phase. We have explored the performance of an extended throat venturi meter with multiple differential pressure measurements under high void fraction conditions. A schematic of the types of devices whose performance is examined is shown in Figure 7. The flow is from left to right.

TEST APPARATUS AND TEST CONDITIONS

Testing has been conducted at nominally atmospheric pressure using air-water flows in a laboratory apparatus at the Idaho National Engineering and Environmental Laboratory and at 400 and 500 psi using dry pipeline natural gas and hydrocarbon liquids in the test fixture shown schematically in Figure 8. Elevated pressure testing was conducted at the Hydrocarbon Training & Development Center in Houston, TX.

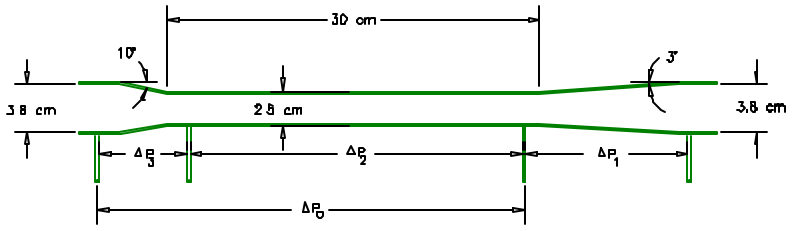

Figure 7. Schematic of extended throat flow nozzle, flow is left to right.

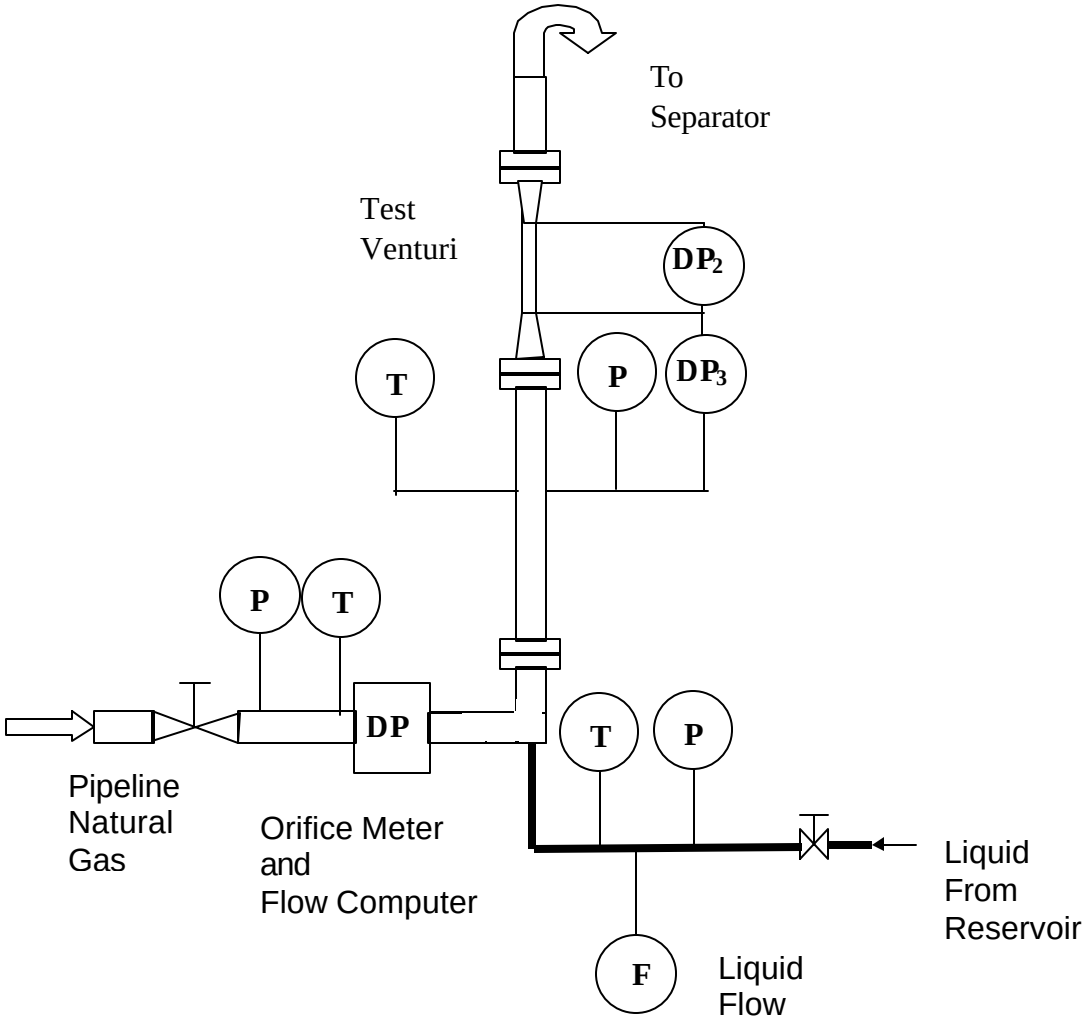

Figure 8. Schematic of test apparatus.

Pipeline natural gas is diverted, metered by an orifice and PECO Corp. Smart Computer, then introduced to the test apparatus at the mixing elbow. Similarly, the test liquid is metered by a turbine meter and a PECO Corp. Smart Computer. The fluid is introduced to the flow stream through a concentric tube in the center of the elbow. All testing was conducted in vertical, upward flow. Test section piping is nominally 2 inch inside diameter. Appropriate pressure and temperature measurements are provided for the single-phase fluids and for the multi-phase mixture just upstream of the test venturi. After flowing through the venturi the gas and liquid

phases are separated, the liquid is re-circulated through the test apparatus and the gas phase is returned to the pipeline.

Three differential pressure measurements are recorded for the extended throat flow nozzle, Figure 7. The measured differentials are ΔP_3 across the contraction, ΔP_2 in the extended throat, and ΔP_0, which should equal $\Delta P_3 + \Delta P_2$, as a consistency check. The complete range of test conditions is summarized in Table 1. Extended throat venturi with two throat diameters and three contraction ratios have been tested over pressures ranging from nominally atmospheric to 500 psi using two gases and four liquids with specific gravity ranging from 0.79 to 1.2.

Table I. Summary of Venturi Geometry and Test Conditions

	INEEL 1" Venturi	PECO 1.4" Venturi	PECO 1" Venturi
Pressure	15 psi	400, 500 psi	400, 500 psi
Fluids	Air-Water Air-Salt Water	*Isopar M â* - Natural Gas	*Isopar M â* *Aromatic 100*- Natural Gas
Liquid specific gravity	1.0 1.2	0.79	0.79 0.87
Throat diameter	1.0 "	1.4 "	1.0 "
Contraction ratio β=d/D	0.656	0.677	0.484
Gas mass flow rate range	0 – 0.015 10^3 lb/min	0 – 0.135 10^3 lb/min	0 – 0.135 10^3 lb/min
Gas volumetric flow rate range	0 – 0.5 10^6 scfd	0 – 4.3 10^6 scfd	0 – 4.3 10^6 scfd
Liquid mass flow rate range	0 – 0.15 10^3 lb/hr	0 – 0.8 10^3 lb/hr	0 – 0.8 10^3 lb/hr
Liquid volumetric flow rate range	0 – 20 bbls/day	0 – 70 bbls/day	0 – 70 bbls/day
Liquid mass loading range m_l / m_g	0 – 30 %	0 – 30 %	0 – 30 %
Estimated void fraction range	0.99 – 1.0	0.94 – 1.0	0.95 – 1.0

ONE-DIMENSIONAL THEORY AND GAS MASS FLOW RATE

One-dimensional theory can not yield an exact description of meter performance, however it can provide insight into the observed behavior under multi-phase conditions. As described in the introduction the gas and liquid phases are strongly coupled. As the gas phase accelerates in the converging section of the nozzle, the denser liquid phase velocity appreciably lags that of the lighter gas phase. In the extended throat region the liquid phase continues to accelerate, ultimately approaching its equilibrium velocity with respect to the gas phase. Even at equilibrium significant velocity differences or slip will exist between the gas and liquid phases. Conservation of mass and energy for each phase is written below where the subscript (1) denotes

the upstream condition and (2) the throat. ΔP_{gl3} is the pressure drop experienced by the gas-phase due to irreversible work done by the gas phase in accelerating the liquid phase between locations 1 and 2. It is assumed that only the liquid phase is in contact with the wall, f_w is the wall friction coefficient and G_c is a geometry factor which accounts for the acceleration of the fluid in the contraction and the surface area of the contraction.

$$m_g = \alpha_1 \rho_g u_{g1} A_1 = \alpha_2 \rho_g u_{g2} A_2$$

$$m_l = (1-\alpha_1)\rho_l u_{l1} A_1 = (1-\alpha_2)\rho_l u_{l2} A_2$$

3) $$P_1 + \frac{1}{2}\rho_g u_{g1}^2 = P_2 + \frac{1}{2}\rho_g u_{g2}^2 + P_{gl3}$$

$$P_1 + \frac{1}{2}\rho_l u_{l1}^2 = P_2 + \frac{1}{2}\rho_l u_{l2}^2 - P_{gl3} + G_c f_w \frac{1}{2}\rho_l u_{l2}^2$$

The gas phase energy equation can be rewritten using the equation for the gas phase mass flow rate, where D is the diameter of the upstream piping, d is the throat diameter, β = d/D is the contraction ratio, and ΔP_3 is the pressure drop across the contraction.

4) $$\Delta P_3 = \frac{1}{2}\frac{m_g^2}{\rho_g \alpha_2^2 A_2^2}\left(1 - \left(\frac{\alpha_2}{\alpha_1}\right)^2 \beta^4\right) + \Delta P_{gl3}:$$

With the approximation that α_1 and $\alpha_2 \cong 1$, the modified orifice equation results.

5) $$\Delta P_3 \approx \frac{1}{2}\frac{m_g^2}{\rho_g A^2}(1-\beta^4) + \Delta P_{gl3}$$

For single-phase flow ΔP_{gl3} is equal to zero and the equation is solved directly for the mass flow rate m_g. In practice, the single-phase result is modified by the addition of an empirical constant C_c which accounts for the true discharge characteristics (non-ideal one-dimensional behavior and friction losses) of the nozzle and Y which takes compressibility effects into account.

6) $$m_{g1f} = \frac{C_c A Y}{\sqrt{1-\beta^4}}\sqrt{2\rho_g \Delta P_3}$$

As shown in the introduction if equation 6 is used under multiphase conditions the mass flow rate of the gas phase can be significantly overestimated. Under multiphase conditions the mass flow rate of the gas phase is given by:

7) $$m_g = \frac{C_{2f}\alpha_2 A_2 Y}{\sqrt{1-\left(\alpha_2/\alpha_1\right)^2 \beta^4}}\sqrt{2\rho_g(\Delta P_3 - \Delta P_{gl3})}$$

where $\alpha_2 A_2$ represents the cross sectional area occupied by the gas phase. For ΔP_3 large with respect to ΔP_{gl3} the quantity under the radical can be approximated by

8) $$\sqrt{\Delta P_3 - \Delta P_{gl3}} \approx \sqrt{\Delta P_3} - C_{gl3} \times \sqrt{\Delta P_{gl3}}$$

where C_{gl3} is a constant to be determined. Empirically we have found that ΔP_{gl3} can be replaced by ΔP_2, the pressure rise in the extended throat, with appropriate choice of constants. The mass flow rate of gas under both single phase and multiphase conditions now becomes

9) $$m_g = \frac{C_{2f} A Y}{\sqrt{1-\beta^4}}\sqrt{2\rho_g}\left[\sqrt{\Delta P_3} - C_2 \times \sqrt{P}_2\right],$$

where we have assumed that $\alpha_2 \approx \alpha_1 \approx 1$. The constants $C_{2\phi}$ and C_2 have been determined empirically and the validity of the equation has been tested over a wide range of conditions.

Figures 9 and 10 show the 1 inch low pressure air-water mass flow rate data plotted with the 1.4 inch 400 and 500 psi natural gas-Isopar M data. Overall, two throat diameters, 1" and 1.4", representing three contraction ratios, at pressures ranging from atmospheric to 500 psig using two gases, and four fluids have been experimentally examined. A single universal set of constants has been found to yield gas mass flow rates with a accuracy of ± 2 % of reading for liquid mass loading m_l/m_g < 10 % and ± 4 % of reading for 10% < m_l/m_g < 30%. This liquid loading range covers the void fraction range from 0.95< α <1.0, where α is the volume fraction of the gas phase.

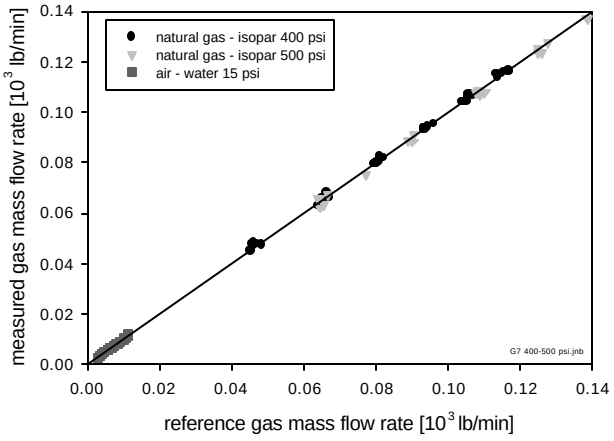

Figure 9. Comparison of measured and reference gas mass flow rates.

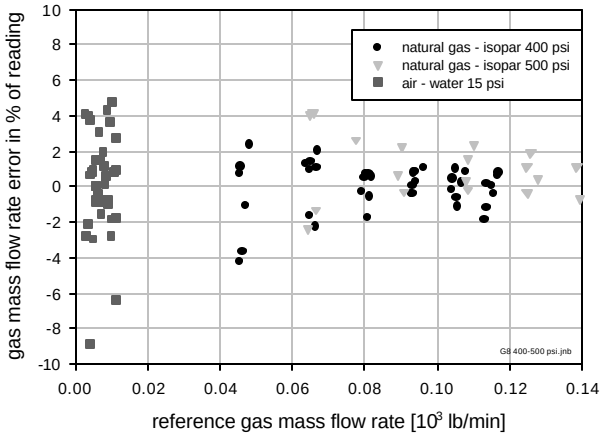

Figure 10. Gas mass flow rate measurement error in percent of reading.

We have assumed that $\alpha_2 \approx \alpha_1 \approx 1$, making equation 9 only approximate. The statistical fitting procedure used to determine the constants $C_{2\phi}$ and C_2 implicitly determines a weighted mean value of α. Hence, because α does not appear explicitly and is unknown there is an uncertainty of ± 1-2 % over the void fraction range 0.95 < α < 1.0, implicit in the equation. If α or (1-α) is independently measured the observed measurement uncertainties can be significantly reduced. The uncertainty can also be significantly reduced if, at installation, the actual flow rates are accurately known. If this measurement is available then the meter reading can be adjusted to reflect the true value and the uncertainty in the gas phase mass flow rate measurement can be reduced to less than 0.5 % of reading if the flow rates change by less than 50% or so over time. The repeatability of the measurement is essentially the random uncertainty in the pressure measurements, less than about 0.5 % of reading.

TOTAL AND LIQUID MASS FLOW RATE

If the ratio of liquid to gas flow rate is known *a priori* with certainty then the mass flow rate of the liquid phase can be directly obtained from $m_l = m_g \left(m_l / m_g\right)_{known}$. Note that because the liquid mass flow rate is only a fraction (0-30%) of the gas mass flow rate the uncertainty in the measurement is magnified. For instance, if m_l/m_g = 0.01, a 1% error in m_g is magnified to

become a 100% of reading error for the liquid phase. An additional fixed error of 1% in the ratio m_l/m_g results in a 200% of reading total error for the liquid phase. This approach, of course, assumes that the m_l/m_g ratio remains constant over time.

Unfortunately, without accurate, independent knowledge of α or $(1-\alpha)$ the liquid mass flow rate cannot be obtained directly from one-dimensional theory. The velocity of the liquid phase can, however, be estimated directly as follows: Once the mass flow rate of the gas phase is determined the ΔP_{gl3} term can be estimated from the gas phase energy equation:

10) $$\Delta P_{gl3} \approx \Delta P_3 - \frac{1}{2}\frac{m_g^2}{\rho_g A^2}(1-\beta^4)$$

Rearranging the liquid phase energy equation yields

11) $$\Delta P_3 + \Delta P_{gl3} = \frac{1}{2}\rho_l u_{l2}^2\left(1-\frac{u_{l1}^2}{u_{l2}^2}\right)+G_c f_w \frac{1}{2}\rho_l u_{l2}^2$$

and using the expression for the mass flow rate of liquid results in

12) $$\Delta P_3 + \Delta P_{gl3} = \frac{1}{2}\rho_l u_{l2}^2\left(1-\frac{(1-\alpha_2)^2}{(1-\alpha_1)^2}\beta^4\right)+G_c f_w \frac{1}{2}\rho_l u_{l2}^2$$

With the assumption that $\frac{(1-\alpha_2)^2}{(1-\alpha_1)^2}\beta^4 << 1$ the liquid velocity u_{l2} can be estimated. If $(1-\alpha)$ is known then the liquid mass flow rate could be estimated directly from $m_l = (1-\alpha_2)\rho_l u_{l2} A$. Unfortunately, $(1-\alpha)$ cannot be accurately estimated from the differential pressure data, it must be independently measured to pursue this approach.

If we consider the gas and liquid phases together but allow their velocities to differ, the total mass flow rate can be written as

13) $$m_t = m_g + m_l = \left(\alpha\rho_g + \frac{(1-\alpha)}{S}\rho_l\right)u_g A$$

where the density term in brackets is the effective density, ρ_{slip}. Since m_t is constant throughout the venturi allows us to write the pressure drop ΔP_3 as

14) $$\Delta P_3 = \frac{1}{2}\left(\alpha\rho_g + \frac{(1-\alpha)}{S}\rho_l\right)u_g^2(1-\beta^4)+G_c f_w \frac{1}{2}\rho_l u_{l2}^2$$

The second term on the right hand side is the friction loss assuming that only the liquid phase is in contact with the wall. The equation can be rearranged to yield the total mass flow rate

15) $$m_t = \left(\alpha\rho_g + \frac{(1-\alpha)}{S}\rho_l\right)u_g A = \frac{2\left(\Delta P_3 - G_c f_w \frac{1}{2}\rho_l u_{l2}^2\right)A}{(1-\beta^4)\cdot u_g}$$

If the assumptions leading to this equation are approximately correct then m_t can be obtained directly from ΔP_3 once u_g is estimated from the measured value of m_g, $u_g = m_g / \rho_g A$ and u_{12} is calculated from equation 12. The results of this calculation for the 400 and 500 psi 1.4-inch venturi data appear in Figures 11 and 12. The friction factor $C_c f_w$ is taken to be 0.062. While the friction term is small it should not be ignored. The total mass flow rate is obtained with a measurement uncertainty of ± 4 % of reading.

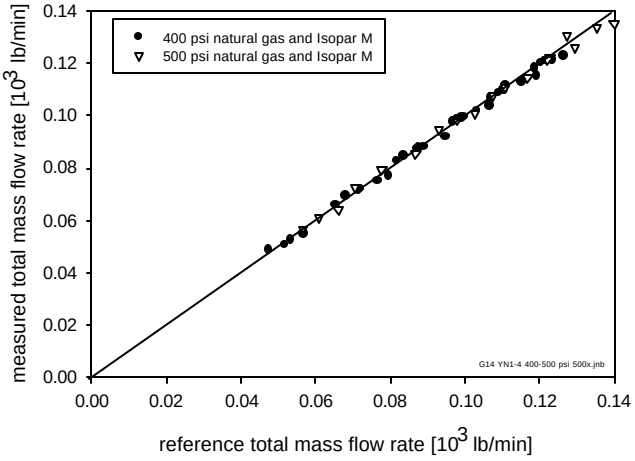

Figure 11. Measured total mass flow rate.

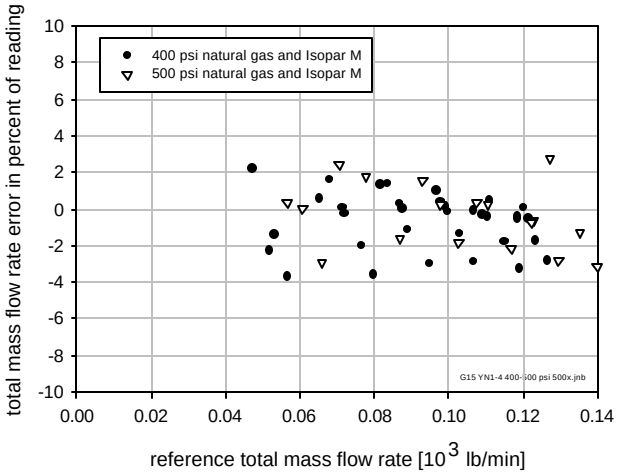

Figure 12. Total mass flow rate error in percent of reading.

In principle, (since the total mass flow rate is the sum of the gas and liquid mass flow rates) the liquid mass flow rate can now be obtained directly from, $m_l = m_t - m_g$. The result of this calculation for the 400 psi data is shown in Figures 13 and 14. When attempting to deduce a small number, m_l, from the difference of two large numbers the resulting uncertainty is also

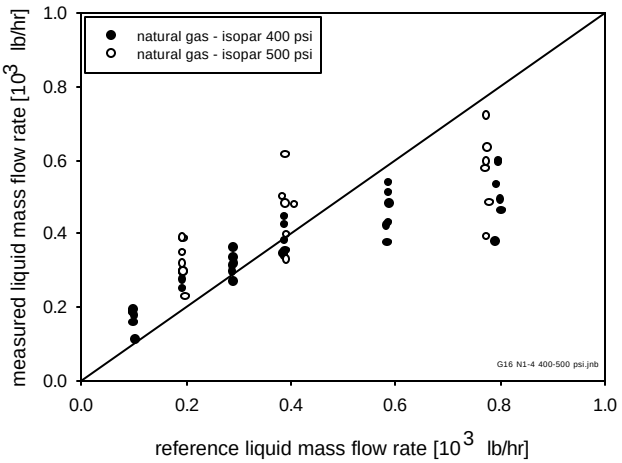

Figure 13. Comparison of measured and reference liquid mass flow rates.

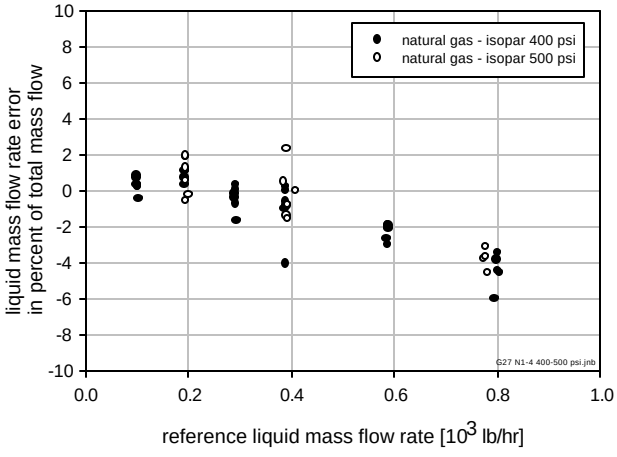

Figure 14. Liquid mass flow rate error in percent of reading of total mass flow rate.

large, this is evident in Figure 13. Realistically this error should be quoted in terms of the total mass flow rate, Figure 14. The liquid mass flow rate can be obtained within ±5% of the total mass flow rate.

INSTALLATION BENCHMARKING

As previously noted in the discussion of the measurement of the gas mass flow rate, if the flow rates of each phase are accurately known at the time of installation, measurement performance over a reasonable range of mass flow rates can be significantly enhanced. The data suggest that the uncertainty in the gas mass flow rate measurement can be reduced to < 0.5 % of reading by benchmarking even if the gas and/or liquid mass flow rates change by ± 50 %. Similarly the uncertainty in the total mass flow rate can be reduced to < 2 % of reading for the same ± 50 % changes in gas and/or liquid mass flow rates. The corresponding improvement in accuracy of the liquid phase measurement is also significant. Because the liquid mass flow rate measurement is dependent on both the gas phase and total mass flow rate measurements (equation 16), the uncertainty is also sensitive to changes in both gas and liquid mass flow rate. If the liquid mass flow rate measurement is benchmarked at an initial value, the data indicate that the accuracy attainable is ±20% of reading for changes in gas mass flow rate in the range of #±15% and/or changes in liquid mass flow rate in the range of #±25%. The uncertainty in the liquid mass flow rate quoted in terms of percent of total mass flow rate becomes ±1%.

CONCLUSIONS

The mass flow rate measurement performance of the extended throat flow nozzle is summarized in Table I below. The uncertainty in the measurement of the mass flow rate of each phase and the total mass flow rate is expressed in percent of reading of the total mass flow rate $m_t = m_g + m_l$. The "benchmarked" columns are specified as both percent of reading of the mass flow rate of the measured phase and percent of reading of the total mass flow rate. Measurement uncertainties can be significantly reduced if flow rates are accurately known at time of meter installation or periodically measured by separation and separate metering during the service life of the meter and the well. Because the liquid phase is only a small fraction of the total mass flow rate the uncertainty in its measurement is inherently high.

Table I. Mass flow rate measurement performance summary.

	Uncertainty in % of total mass flow	Benchmarked uncertainty in % of reading*	Benchmarked uncertainty in % of total mass flow*
Gas phase	± 4 %	± 0.5 %	± 0.5%
Total mass flow	± 4 %	± 2 %	± 2 %
Liquid phase	± 5 %	± 20 %	± 1 %

* see section on "INSTALLATION BENCHMARKING"

ACKNOWLEDGMENTS

This work was performed under the auspices of the U.S. Department of Energy under DOE field Office, Idaho, Contract DE-AC07-94ID13223. Support was provided by Laboratory Directed Research and Development funds and by Perry Equipment Corporation.

REFERENCES

1) Hewitt, G. F. (1998) Differential Pressure, Dual Energy Gamma Densitometry and Cross Correlation in Multiphase Flow Measurement, International Conference on the Future of Multiphase Metering, London, UK.
2) Avallone, E. A. and Baumeister (1987). Mark's Standard Handbook for Mechanical Engineers, McGraw Hill, New York, pp. 3.62 – 2.63.
3) Murdock, J. W. (1962). Two Phase Flow Measurement with Orifices, ASME Journal of Basic Engineering, December, 419-433.
4) Jamieson, A. W. and Dickinson, P. F. (1993). High Accuracy Wet Gas Metering, Proceedings, North Sea Flow Measurement Workshop, Bergen, Norway.